Naval Research Laboratory
Washington, DC 20375-5320

U.S. NAVAL RESEARCH LABORATORY

NRL/5620/MR—2021/2

A Review of Reactive Ion Etching of Glass Materials

AUSTIN F. MOORE

Jacobs, Inc.
Hanover, MD

JESSE A. FRANTZ

LYNDA E. BUSSE

JASBINDER S. SANGHERA

Optical Materials and Devices Branch
Optical Sciences Division

October 4, 2021

REPORT DOCUMENTATION PAGE

Form Approved
OMB No. 0704-0188

1. REPORT DATE *(DD-MM-YYYY)*	**2. REPORT TYPE**	**3. DATES COVERED** *(From - To)*
04-10-2021	NRL Memorandum Report	10/01/2012 – 09/30/2021

4. TITLE AND SUBTITLE

A Review of Reactive Ion Etching of Glass Materials

5a. CONTRACT NUMBER
N00173-14-D-2023

5b. GRANT NUMBER

5c. PROGRAM ELEMENT NUMBER

6. AUTHOR(S)

Austin F. Moore*, Jesse A. Frantz, Lynda E. Busse, and Jasbinder S. Sanghera

5d. PROJECT NUMBER

5e. TASK NUMBER

5f. WORK UNIT NUMBER
6B49

7. PERFORMING ORGANIZATION NAME(S) AND ADDRESS(ES)

Naval Research Laboratory
4555 Overlook Avenue, SW
Washington, DC 20375-5320

Jacobs, Inc.
7740 Milestone Parkway
Hanover MD, 21076

8. PERFORMING ORGANIZATION REPORT NUMBER

NRL/5620/MR--2021/2

9. SPONSORING / MONITORING AGENCY NAME(S) AND ADDRESS(ES)

Naval Research Laboratory
4555 Overlook Avenue, SW
Washington, DC 20375-5320

10. SPONSOR / MONITOR'S ACRONYM(S)
NRL

11. SPONSOR / MONITOR'S REPORT NUMBER(S)

12. DISTRIBUTION / AVAILABILITY STATEMENT

DISTRIBUTION STATEMENT A: Approved for public release; distribution is unlimited.

13. SUPPLEMENTARY NOTES

*Jacobs, Inc., 7740 Milestone Parkway, Hanover, MD 21076

14. ABSTRACT

This report explores the published parameters for reactive ion etching (RIE) of various types of glassy materials, including those used to fabricate random antireflective surface structures (rARSS). The glasses included in this report are fused silica, borosilicate glass, aluminosilicate glass, as well as chalcogenide and phosphate glasses.

15. SUBJECT TERMS

Antireflective surface structures
Glass etching
ARSS
Nanostructured surfaces
Moth eye

16. SECURITY CLASSIFICATION OF:			**17. LIMITATION OF ABSTRACT**	**18. NUMBER OF PAGES**	**19a. NAME OF RESPONSIBLE PERSON**
					Jesse Frantz
a. REPORT	**b. ABSTRACT**	**c. THIS PAGE**	U	50	**19b. TELEPHONE NUMBER** *(include area code)*
U	U	U			(202) 767-9519

Standard Form 298 (Rev. 8-98)
Prescribed by ANSI Std. Z39.18

This page intentionally left blank.

CONTENTS

This page intentionally left blank.

1. INTRODUCTION

The aim of this report is to explore the published parameters for reactive ion etching (RIE) of various types of glassy materials, including those used to fabricate random antireflective surface structures (rARSS). The glasses included in this report are fused silica, borosilicate glass, aluminosilicate glass, as well as chalcogenide and phosphate glasses. One of the primary processes for forming surface structures on glasses is through reactive ion etching with the use of inductively coupled plasma (ICP). In this report, the published mechanisms of ICP and RIE will be examined, and conditions and parameters used to obtain strong etching rates with low levels of isotropy will be discussed. The parameters that are of particular interest are ICP RF power, bias voltage/power, pressure of the chamber, types of processing gases, and gas flow rates. We will include published work on parameters for fabricating rARSS on various types of glasses. Finally, a discussion of the results will be presented with general trends shown that have optimized the etching processes on various glasses.

2. FABRICATION MECHANISMS

RIE is a type of dry etching that is used for its unique ability to etch anisotropic structures on the surface of a material. Dry etching is the process whereby a gas plasma is used to remove material from the surface of a target. Dry etching performs this function by introducing gaseous radicals that adsorb to the surface of the target but do not have the chemical potential to create a volatile byproduct that will spontaneously remove itself from the surface. This process is later activated, to the specifications of the user, by using ions to bombard the surface and induce a chemical reaction. The ions within the plasma act as a catalyst that breaks the bonds of the atoms on the surface of the target, which in turn allows the radicals to bond with the surface atoms and create a volatile product, which then is removed from the surface. Because of the structure of the machine and the directionality of the plasma, the majority of ions approach the surface only

Manuscript approved September 30, 2021.

in a vertical direction, allowing for etches with a high degree of anisotropy, that is to say a highly vertical profile of the sidewalls [1].

The ion-assisted chemical reactions at the surface are the main mechanism whereby etching occurs. However, there are other factors that must be taken into consideration in order to fully understand how various parameters affect the etching rate. In addition to assisting the chemical etching process, the ions also have the effect of physical sputtering upon the surface. Thus, process gases such as Ar will perform this double effect. In most cases, though, there is also another process gas such SF_6, CF_4, CHF_3, or C_4F_8. This gas is also partially ionized and will contribute to the physical etching in addition to its primary role as a chemical etchant [1].

Typical RIE machines employ capacitively coupled plasma (CCP) technology to create a plasma which will then send ions onto the surface. A CCP machine uses an RF power source to send an oscillating current through a pair of parallel plates which produces a field that affects the movement of the electrons and ions in vastly different manners. The electrons will accelerate quickly between the top and bottom plates, while the more massive positive ions accelerate much more slowly. The result of this effect is the formation of a plasma which is utilized so as to bombard ions at the etching targets [1].

A major limitation of CCP technology is that there is only one source of RF power, which does not allow for a variation of parameters. Effectively, the power supply is used to both generate the plasma and accelerate the positive ions at the boundary layer of the plasma, also known as the sheath. This can also be thought of as the RF power supply being used to control the density and the effective energy of the plasma [1].

This limitation can be worked around with a more advanced technology, which is ICP. This technology makes use of toroidal coils and RF currents to induce a separate toroidal shaped formation of plasma. In

this configuration, the primary RF current is used only to generate the plasma and to control its density. Unlike in the CCP configuration, at the location in which the plasma is generated, there is not a RF current that passes through capacitive plates that would determine the ion energy in addition to the plasma density. Instead, a plate that holds the target is placed under the ICP device so that the plasma may be uniformly distributed upon the target. To this plate, another separate RF supply may be connected that will determine the ion energy by accelerating the ions in the sheath. In this configuration, then, the parameters of plasma density and energy can be controlled separately. In effect, this allows for more highly dense plasmas while also allowing for a larger window of ion energies [1].

It must be noted that there are some specific terms that can be used equivocally among CCP and ICP technologies. When speaking of the power generated using the RF source in CCP, the term that will be used henceforth will be “source power”. When speaking of the primary RF source to power the coils in ICP, the term will be “coil power”, and the term for the separate RF source connected to the plate will be called the “platen power”. Lastly, “bias voltage” is a term that is used differently in these two technologies, due to the difference in how this voltage is formed. In CCP, a voltage is formed between the capacitive plates in the device, and this is often called “self-bias voltage”. This is often confused with a separate quantity “bias voltage”, which is the sum of self-bias voltage and the plasma potential. In reality, there is little difference between bias voltage and self-bias voltage since the plasma potential is so small in comparison to self-bias voltage. This term is further complicated when it is used in reference to ICP, since the voltage is controlled directly by a separate RF power source. In the studies presented, the terms will be used interchangeably, but one should be aware of these differences.

Having a general understanding of both RIE and ICP, it can now be more fully understood how one may vary the parameters of these processes to achieve a particular set of structures on the surface of the sample target. Every sample will require different parameters to achieve the same structure, both because of chemical composition of the material as well as the physical structure. For example, the process to make

"moth eye" structures (having fixed height and spacing) on a crystalline material is very different than the process to form these same structures on an amorphous material.

3. RIE OF VARIOUS GLASSES

3.1 Silica Based Glasses

3.1.1 Fused Silica

Fused silica is a glass that does not contain any impurities or any other components, being made up only of silicon and oxygen. Because of its simplicity, it is a quite straightforward process to etch it. However, silica's simplicity has also made it a prime candidate for RIE, which in turn has produced diverse methods to accomplish the same goal. A variety of processing gases may be used, and these gases may be introduced at very different flow rates and at different working pressures.

A study was conducted by Patrick Leech [2] in 1999 to determine suitable parameters for etching silica-based glasses. In this study, the researchers performed experiments of RIE on these glasses using CCP technology rather than ICP. It is for this reason that there will only be references to the main source power, with no consideration given to a secondary platen power. In this study they addressed etching of both high purity silica glass (Suprasil) as well as other varieties of fused quartz. Granted that the impurity content may differ between these materials, the general results of this study can still be used, given that the nominal chemical compositions are identical.

Initially in this study a limited number of parameters were fixed. The experiments were done in vacuum, with the base pressure of the chamber fixed at 4.5×10^{-4} mTorr, the backside temperature maintained at 20° C, and the mass flow rate of the processing gas fixed at 25 sccm. With these given conditions, a series of

experiments were conducted to determine optimal parameters to best increase etching rate while also maintaining a high degree of anisotropy. First, a series of experiments was done to determine the optimal power, and thus ion energy, to achieve high etching rates. In another series of experiments, the ratio of processing gases of CHF_3/CF_4 was varied to determine the best ratio for the RIE of silica. Lastly, a final round of experiments was conducted with Ar as a purely physical sputtering process to compare results with an ion assisted chemical etching.

The source power of the RIE process was measured by the value of the bias voltage. The data showed that the etch rate was dependent on the square of this voltage. To be clear, bias voltage is nothing other than the voltage created between the plasma sheath and the plate that holds the sample. This led the authors to create plots that showed the etch rate against the square root of the voltage, as is seen in Figure 1.

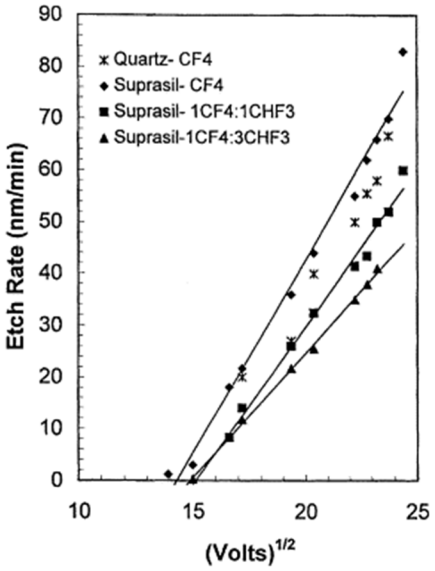

Fig. 1 — Plot of etch rate as a function of bias voltage [2]

Focusing on the data points for quartz, it can be observed that etch rate increases at a constant rate as the bias voltage increases. From this data, one can infer that etching rate is largely dependent on power, and thus an increase in power will always result in an increase in etch rate. In later studies, though, it was shown

that higher powers significantly increased undercutting of the etch, which is a serious detriment to anisotropy. Therefore, source power should be increased as high as can be possibly tolerated without affecting the required sidewall angle and anisotropy that is desired for a particular etching.

An investigation of the effect of gas ratios of CHF_3/CF_4 was conducted and also compared to a process in which only Ar is used. From these comparisons it was found that silica was most quickly etched by CF_4 alone. Any increase of the ratio of CHF_3 to CF_4 was found to only decrease the etch rate. This indicates that CHF_3 is a less effective etchant of silica. When comparing these fluorine based processing gases to Ar, it was found that Ar was far less effective than either CF_4 or CHF_3. The author credited this to argon's inert character and that its ability to etch came only from physical sputtering with no regard towards assisting in any form of a chemical process [2].

Another study, by Schmitt et al [3], was conducted in 2018 that closely followed the study performed by Leech [2], whereby the authors attempted to study the effects of each parameter on the etching rate of several types of silica based glasses using CCP RIE. Many of these results are nearly identical to those of the last study. However, there is also a difference in the processing gases used, which sheds light on how to improve the etching rate of silica based glasses.

There are two main results of this study. For both of the current and previous study, it is notable that pure silica always has the greatest value of etching for each variation of parameters, and it always has the greatest rate of change as each parameter varies. Silica based glasses that contain other components often result in a slower etching process with a higher level of isotropy. This will be covered in greater detail later, but it must be kept in mind as the following observations are described.

The first observation of the Schmitt et al. study was that the pressure of the chamber is inversely proportional to the etching rate. This relationship is shown in Figure 2.

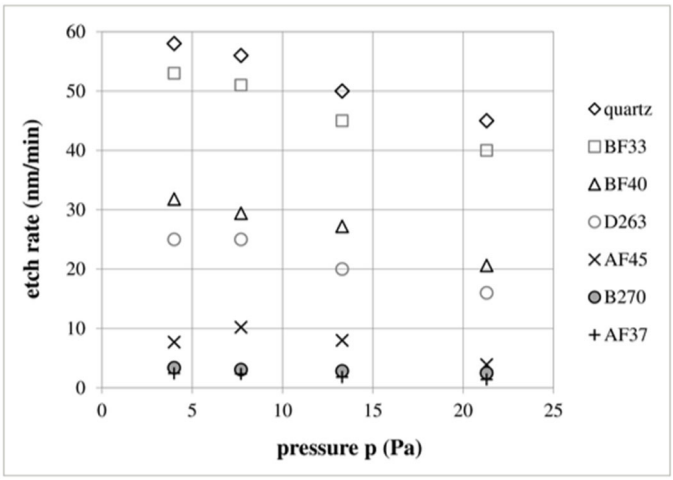

Fig. 2 — Etch rate as a function of pressure [3]

The ideal pressure would appear to be as close to vacuum as possible. It must be admitted, though, that the pressure cannot be so low that the plasma density would altogether disappear. The lowest you can bring the pressure without completely sacrificing the plasma density must then be the ideal pressure to maximize etch rate. According to this study, a pressure of 4 Pa or 30 mTorr would be exemplary.

The most interesting result of this study is the conclusion that a mixture of a fluorine based gas is most effective when it is combined with argon, in order to enhance the etching through both physical and chemical means.

Unlike the previous study by Leech, whereby there was a comparison of various mixtures of CF_4/CHF_3 and then separate experiments using Ar, in this study a mixture of CF_4 and Ar was used. CHF_3, consistent with being a less effective processing gas for silica based glasses, was not used for any of these trials. The addition of Ar, however, enhanced the effect of etching when it consisted of nearly 30% of the total mass flow of processing gas, as is shown in Figure 3.

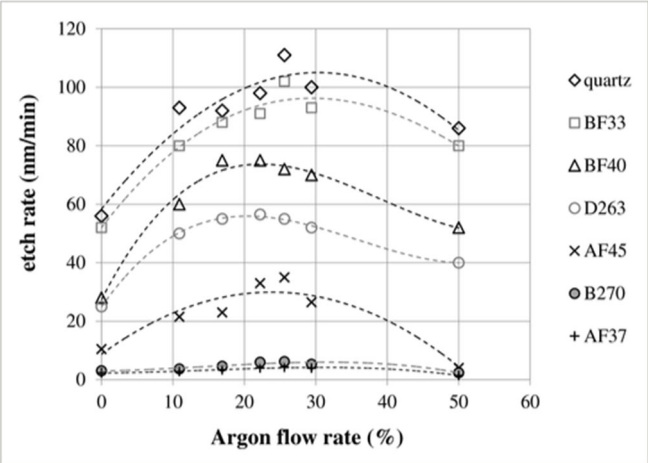

Fig. 3 — Etch rate as a function of argon flow rate [3]

Having performed all of the necessary trials, the authors of this study suggest that the source power be at a value of 270 W. The pressure was recommended to be low, around 30 mTorr. Together, these parameters result in a desired bias voltage of -585 V. Finally, it was shown that a mixture of CF_4 and Ar was extremely effective at etching silica. The total flow rate shown to be most effective was a mixture where CF_4 was input at 20 sccm and Ar at 10 sccm. Together, these were concluded as the optimal conditions for RIE of silica

The following passage from the study gives an excellent summary of combining Ar and CF_4 in the processing plasma: “The etch rates were increased for all glass samples using an additional Ar content in the plasma. They reached a maximum for Ar flow rates between 10 and 20 sccm, which corresponds to a CF_4/Ar flow rate of about 3:1. Etch rates increased by a factor of 2 (quartz, BF33) up to a factor of 3.5 (AF45) compared to the pure CF_4 plasma. For Ar flow rates higher than 20 sccm, an etch rate decrease was observed. These results are interpreted in terms of the two recognized processes of ion-enhanced chemical etching and physical sputter etching. Obviously the additional Ar component in the CF_4/Ar mixture promotes the formation of reactive CF_x radicals and, consequently, increases the ion-enhanced chemical

etching for the 'pure' SiO_2 (quartz) and the sample with the lowest alkaline content (BF33). Furthermore, the physical sputtering of nonvolatile alkaline and alkaline byproducts by Ar ions causes a continuous removal of these species from the etched glass surface. Without this sputter process the alkaline and alkaline-earth byproducts are enriched at the glass surface during increasing etching time and thus they reduce the etch rate considerably. For pure CF_4 plasma (in absence of Ar ions), decreasing etch rates were measured on the surfaces of the alkaline-rich and alkaline-earth-rich glasses (AF45, D263, B270, AF37) with increasing etch time. In case of the gas mixture with identical CF_4 and Ar flow rate (50% each at 24 sccm) the surface collision rate of the CF_x radicals is considerably reduced by the argon share in relation to the Ar collision rate. Therefore, the chemical reaction rate at the surface drops, which leads to a diminished overall etch rate." [3].

A third study was conducted in 2018, by Zhang and Tadigadapa [4], using a modified ICP-RIE system. In this setup, the primary processing gas was SF_6, used to generate the plasma. In addition to this, though, there were two diffuser rings set up near the wafer target which introduced NF_3 and H_2O vapor. The flow rate of each of these gases was independently controlled so as to determine the optimal mixture for RIE of various silica based glasses.

Before conducting any of their own research, the authors of this study first began by displaying the results of a bulk of the previous major studies performed using ICP-RIE, so as to give a general overview of the relative etch rates achieved in the past. These results (in Tables 1 and 2) will prove as invaluable assets, as they may serve as a basis from which the optimal values of the parameters may be inferred.

Table 1 — Recorded Etch Rates of Silica [4]

Reference	Etch Rate (μm/min)	Roughness (nm)	Mask Material	Selectivity	Etched Depth (μm)	Aspect Ratio	Glass Type
Abe et al., 1999 [6]	0.5	2	Nickel	30	20	0.05	Quartz
Li et al., 2000 [7]	0.5	N/A	Nickel	N/A	N/A	N/A	Fused silica
Chen et al., 2001 [8]	0.55	N/A	Nickel	N/A	N/A	N/A	Fused silica
Queste et al., 2010 [9]	0.74	N/A	Nickel	27	13	2.9	Quartz
Zhang et al., 2014 [10]	1	0.5	Nickel	16	102	5.2	Fused silica
Ahamed et al., 2015 [11]	0.35	38	Nickel	70	70	7	Fused silica

Table 2 — Processing Details of Silica Etches

Reference	Etch Rate (μm/min)	Processing Gas	Flow Rate (sccm)	Coil Power (W)	Platen Power (W)	Pressure (mTorr)	Temperature (ºC)
Abe et al., 1999 [6]	0.5	SF_6	N/A	150	-340 V (Bias Voltage)	1.5	20
Li et al., 2000 [7]	0.5	SF_6	N/A	150	N/A	1.5	N/A
Chen et al., 2001 [8]	0.55	N/A	N/A	1000	N/A	1.5	N/A
Queste et al., 2010 [9]	0.74	C_4F_8/O_2	N/A	N/A	600	8	N/A
Zhang et al., 2014 [10]	1	$SF_6+(NF_3+H_2O)$	60/100/50	2500	400	4.5	N/A
Ahamed et al., 2015 [11]	0.35	C_3F_8/Ar	30/60	N/A	N/A	N/A	-10

The fastest etch rate on Table 3 was achieved by Zhang and Tadigadapa [4], the author of this current study, using a configuration similar to what was described above. The authors state: "Using this configuration ($SF_6/NF_3/H_2O$ mixture), source [coil] power of 2500 W, substrate [platen] power of 400 W, and $SF_6/NF_3/H_2O$ flow rates of 60/100/50 sccm, we were able to achieve a surface roughness of ~5 Å at an etch rate of ~1 μm/min." [10]. Following close behind with similar results, the setup of the Queste study was stated as such: "Best results were obtained using a pressure of C_4F_8/O_2 plasma of 8 mTorr with a [coil] power of 600 W and an 8 μm thick electrodeposited Ni etch mask. A depth of up to 120 μm with an aspect ratio of 20 was achieved with an etch rate comprised between 0.7 and 1 μm/min depending on the size of the structures, an etch selectivity of 18:1, and angles of 83°–88°." [9]

The Zhang and Tadigadapa study [4] aimed to increase etch rates from these already promising results, both in silica itself as well as borosilicate and aluminosilicate glasses. All glasses were etched under the following conditions: the wafer was placed 120 mm from the plasma source, coil power was set to 2000 W and the platen power was set to 400 W, pressure was set to 4 mTorr, the backside was cooled with He to a constant 20^o C, and a gas inflow rate of SF_6:NF_3:H_2O::20:20:25 sccm. Again, it must be noted that only the SF_6 was properly ionized as a plasma, whereas the NF_3 and H_2O were only partially ionized during the process, if at all. With these conditions, it was reported that the silica was etched at a rate of 1.06 μm/min with a smoothness of 2 Å.

The authors of this study criticize the conventional use of a mixture of a fluorine radical and argon, especially when etching glasses that are not purely silica. They state: "Etches performed at lower pressure are expected to be dominated by higher physical contribution. However, the overall gains are mitigated by the lower flux density of the bombarding ions. This can explain the lower etch rates obtained at low pressures. In contrast, at higher pressures the flux of ions and radicals are increased although the energy of the impinging ions is reduced. This changes the etching mechanism from a physically dominated process

to a chemical process. However, for the chemical process to be effective, sensitization of the surface atoms via bombardment by energetic ions is critical. Since at higher pressures, ion energies are reduced, this results in a less than optimal chemical process thereby reducing the etch rates at the high flow rates." They are stating that there is an irreconcilable need for both chemical and physical processes in order for etching to be optimal, but this requires both high and low pressures of the processing plasmas, which is impossible. Therefore, they conclude that a modified system, with NH_3 and H_2O vapors being introduced near the samples during processing, must be used in order to work around this difficulty [4].

Finally, a fourth study was conducted in 2015 with the direct intent to etch silica substrates to form antireflective surface structures (ARSS). These structures were made in an ordered pattern with a small masking layer of polystyrene nanoparticles. This study seemed to emphasize using slow etch rates with low power conditions in order to better etch the surface properly to form ARSS. This study reported an etch rate of only 0.05 μm/min using the following conditions: coil power of 100 W, pressure of 9 mTorr, 10:1 Ar/CHF_3 flow, 150 sccm Ar and 15 sccm CHF_3. This study did not yield deep etching results, but it is being noted for its attempt to etch silica to form ARSS. This work will be examined more closely later in the study, to fully illuminate why a process such as this may be beneficial in forming ARSS [5].

3.1.2 Soda Lime Glass

Soda lime glass is one of the most commonly used glasses for all purposes. It is composed of three main components: SiO_2 (~70%), Na_2O (~15%), and CaO (~13%). There can be several other additive components that may drastically affect the mechanical and thermal properties.

A relevant study on the etching of soda lime glass was done in 2007, written by Vieillard et al. [12]. It begins with a description of what is necessary to etch glasses that are not pure silica: "Since SiO_2 is the principal component of glasses, the selection of process gases is aimed at this compound. Hence, fluorine-

based plasmas, with SF_6, CF_4, CHF_3 and alike – are typically applied. However, in order to improve the anisotropy of the process by reducing lateral under-etching, the addition of chemically neutral species, typically argon, is indispensable. Argon ions are accelerated by self-bias voltage, thus enhancing the vertical etching rate. Ion bombardment is of particular importance when soda-lime substrates are etched. This material contains a relatively high number of additives that form non-volatile compounds during the process which in turn deteriorate the surface quality and decrease the etching rate. Therefore, the presence of argon ions, which enhance the removal of the material by means of physical sputtering, is crucial here." [12]

The previous 1999 Leech study [2] again points to this same claim, that physical sputtering is the primary process that takes place on soda lime glass. When testing the CF_4/CHF_3 mixture ratios, it was found that varying the composition of the processing gas did not have a significant effect on the etching rate. This clearly suggests that physical sputtering is the dominant process of etching in their experiments. This is due entirely to the fact that the additional components in soda lime glass do not form volatile compounds with the fluorine based radicals and therefore prevent significant amount of chemical reaction to occur.

The Schmitt et al. study [3] again showed that soda lime glass was subject to low etching rates regardless of what ratio of CF_4/Ar was used. In addition to the results from the Leech research [2], they also added that there were instances of surface roughness and micro trenching. This roughness was about 8 nm when using pure CF_4 and 5 nm when using a CF_4/Ar mix. Trenches of about 500 nm also occurred because "physical sputtering by Ar ions is the crucial etching mechanism for removing the nonvolatile alkaline and alkaline-earth atoms, the increased ion density promotes the elimination of these atoms preferably at the edges of the etch groves." It is this phenomenon that the authors claim causes these trenches.

3.1.3 Borosilicate and Aluminosilicate Glass

Borosilicate glass is renowned for its chemical durability, mechanical strength, and thermal properties. It is made up of SiO_2 (~80%), B_2O_3 (~9-13%) as well as some combination of Al_2O_3, alkaline oxides, and alkaline-earth oxides. Common commercial borosilicate glasses include Schott B270, D263, BF33, and BF40. Aluminosilicate glass is similar to the composition of borosilicate glass, but it also contains a large percentage of Al_2O_3, usually >10%. Aluminosilicate glasses of consideration here include Schott AF37 and Schott AF45.

Below, in Table 3, is a list that was presented in the study performed by Schmitt et al. [3] that gives a detailed description of the constituents that are present in various borosilicate and aluminosilicate glasses that are being spoken of presently.

Table 3 — Contents of Borosilicate and Aluminosilicate Glasses (in wt%) [3]

Glass Type	**SiO_2+B_2O_3**	**Al_2O_3**	**Alkaline (Na_2O/K_2O)**	**Alkaline earth (MgO/CaO/SrO/BaO/ZnO)**
Silica	100.00%	0.00%	0.00%	0.00%
BF33	93.30%	2.00%	4.00%	0.00%
BF40	85.30%	>2.00%	>5.00%	>4.00%
D263	65.70%	>6.00%	>15.00%	>7.00%
B270	69.50%	0.00%	>16.00%	>13.00%
AF37	65.00%	>17.00%	0.00%	>16.00%
AF45	63.70%	>11.00%	0.00%	>24.00%

Borosilicate glass is more suitable for etching than soda lime glass or aluminosilicate glass because fluorine based plasmas create volatile compounds when they react with boron oxide. BF_3 is a common compound that forms during RIE reactions that is easily removable from the surface of the substrate.

Below are two tables that present a history of reported ICP-RIE etches of borosilicate glasses. Table 4 gives details of the results of the etching processes and Table 5 is our summary of the reported parameters that were used to achieve these results.

Table 4 — Recorded Etch Rates of Borosilicate Glass [4]

Reference	Etch Rate (μm/min)	Roughness (nm)	Mask Material	Selectivity	Etched Depth (μm)	Aspect Ratio
Li et al., 2000 [7]	0.6	4	Nickel	20	100	10
Ichiki et al., 2003 [13]	0.8	N/A	Chromium	23	32	2
Park et al., 2005 [14]	0.75	N/A	Nickel	N/A	27	2
Akashi et al., 2006 [15]	0.55	N/A	Silicon	6.6	430	0.43
Jung et al., 2006 [16]	0.65	N/A	Nickel	N/A	20	2
Goyal et al., 2006 [17]	0.54	2	Nickel	N/A	33	1.65
Kolari, 2007 [18]	0.6	N/A	Silicon	3.9	330	1.6
Queste et al., 2010 [9]	0.9	30	Nickel	18	120	6
Ahamed et al., 2015 [11]	0.45	62	Nickel	N/A	80	8

Table 5 — Processing Details of Borosilicate Etches

Reference	Etch Rate (μm/min)	Processing Gas	Flow Rate (sccm)	Coil Power (W)	Platen Power/Voltage	Pressure (mTorr)	Temperature (°C)
Ichiki et al., 2003 [13]	0.8	SF_6/Ar	200 (Total)	500	N/A	10	N/A
Park et al., 2005 [14]	0.75	SF_6 or SF_6/Ar	200 (Total)	1100	-500 V	18	N/A
Akashi et al., 2006 [15]	0.55	C_4F_8/CHF_3	5-40	600-900	250- 400 W	1.5-4.5	-20
Jung et al., 2006 [16]	0.65	SF_6/Ar	20 (SF_6) 10 (Ar)	2500	N/A	5	N/A
Goyal et al., 2006 [17]	0.54	SF_6/Ar	50/50	2000	475 W	<2	N/A

Kolari, 2007 [18]	0.6	C_4F_8/He	25/50	1100	-2000 V	N/A	N/A

Optimal conditions for etching borosilicate glass can be gathered from this data. First, it is necessary that both a fluorine-based plasma be used along with an inert glass, such as argon. This must be emphasized as a necessity for these types of glasses, rather than an enhancing factor as it may be with pure silica. As is stated in the Zhang study, "The non-volatile oxides of the dopant atoms in borosilicate glass need energetic ions to be sensitized and subsequent removal through fluorine based chemical reactions." [4] Since the products that are formed from the plasma and the substrate do not have boiling points near the temperatures typical of these experiments, they do not spontaneously depart from the surface. Therefore, it was found that utilizing physical sputtering of argon is necessary throughout the procedure.

It was also observed that the coil power must be relatively high, around 1100 W. Along with this, the pressure of the chamber must be at a sufficiently low level, at least <20 mTorr. Both of these conditions affect the self-bias voltage, which taken together induce a voltage of around -500 V.

Thus, since the self-bias voltage is correlated to the chamber pressure and the coil power, it was then helpful to relate this parameter to the etching rate.

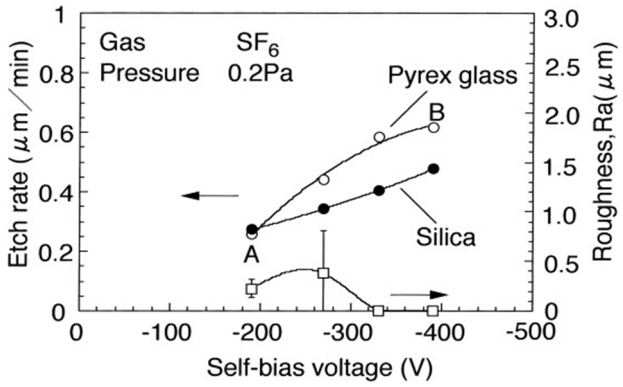

Fig. 4 — Etch rate and roughness of glass substrates as a function of self-bias voltage [7]

As can be seen in Figure 4, the etching rate increases with an increase in self-bias voltage [7]. In addition to this, the roughness of the substrate also increases with voltage. It must be admitted that correlating the self-bias voltage with the etch rate and roughness does not give a full picture of the conditions necessary for those exact rates, since the bias voltage is a function of the pressure and power. This does, however, provide a starting point for determining what pressures and power combinations may be most conducive to effective RIE processes.

It should be pointed out that under most conditions, roughness may prove to be a serious issue. However, in cases of forming rARSS, this may lead to more optimal results. In another section of this same study, the author shows needle-like structures that are formed when placed under the relatively high pressure of 12 mTorr, as can be seen in Figure 5.

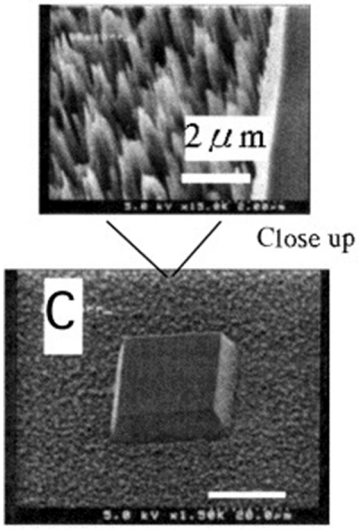

Fig. 5 — SEM images of needle-like structures under high pressure conditions [7]

These trials have given a good sense of the conditions necessary to optimize the etching rate of borosilicate glass. The last study mentioned was particularly interesting because it showed how roughness, a factor that

is normally undesirable for these etching procedures, could potentially be maximized so as to contribute to forming rARSS.

Further reports of ICP-RIE of borosilicate glass list small variations of opinion concerning the coil power, pressure, and platen power [7, 14, 15, and 16]. To summarize, all of these studies [4, 13, 14, 15, 16, 17, 18] show that a fluorine based gas is effective (CF_4, C_4F_8, SF_6) because they react well with SiO_2 and B_2O_3 and because the products are quite volatile (SiF_4 and BF_3). It is other components in the glass, such as alkali metals and alkali-earth metals, that poses a problem since they form products such as AlF_3, NaF, KF, or BaF_2. All of these products are nonvolatile, possessing boiling points well over 1000ºC [4, 13, 14, 15, 16, 17, and 18]

It is the aim of the RIE processes described to remove these volatile products with chemical reactions and little ion bombardment assistance and to remove the nonvolatile products with physical sputtering. For example, if a CF_4/Ar mixture was chosen as the plasma etchant, then CF_4 would form CF_3^+ ions and Ar would form Ar^+ ions that would physically bombard the surface of the target. While this was occurring, CF_2 and CF_3 radicals would be undergoing chemical reactions to form the aforementioned products. These processes can interfere constructively when the bombardment removes some nonvolatile species that cannot be removed through a chemical reaction alone. However, these processes can also interfere destructively, such as when the ions back scatter these nonvolatile compounds back onto the surface of the target. This allows for the formation of clusters of these compounds, which then in turn mask the material from being further etched [19]. Thus, in the report by Schmitt et al., it can be seen that there is a simple correlation between the composition of the glass and the etching rate. The more alkaline and alkaline-earth oxides that are present within the given glass, the slower the etch rate will be. This result is true regardless of the presence of a noble gas, such as argon, within the plasma [3].

3.2 Exotic Glasses

It is worth noting the parameters necessary to use ICP-RIE on more unusual glasses such as chalcogenide glass, phosphate glass, or lanthanum containing glasses. These glasses have more peculiar properties that make them suitable for particular applications, such as IR optical communications.

3.2.1 Chalcogenide Glass

Chalcogenide glasses can vary widely in their composition. For the most part, though, they exist in binary and ternary compounds with group IV and VI elements. The research conducted on RIE processes on chalcogenide glasses is very limited. A study performed by Xiong et al [20] that focuses on deep RIE of $Ge_{20}Se_{75}Sb_5$ films is very enlightening as to how to etch chalcogenide glasses.

The first issue that is discussed in this study is choosing an appropriate processing gas for $Ge_{20}Se_{75}Sb_5$. The authors consider chloride and fluoride based gases. Chlorine based gases are quickly dismissed, though, because of their low selectivity rates. CF_4 and CHF_3 are quickly highlighted as ideal candidates for etching chalcogenide glasses because they form CF_x radicals which create passivation layers on the sidewalls of the formed structures. This, then, allows for superior vertically etched profiles.

The authors state that previous studies have found that CF_4 is a very potent chemical agent on various other chalcogenide glasses. They state that it etches at an extremely high rate of 2 μm/min and leads to a large degree of undercutting and surface roughness. CHF_3 was then chosen as a more suitable source plasma. In addition, it was also investigated as to whether an inert gas would be helpful in diluting the chemical potency of the fluoride gas. Both Ar and O_2 were investigated for their performance in etching plasma

together with CHF_3. It was found that O_2 was actually superior in diluting the reactivity of the fluoride while also showing better results for vertical profiles of the etched structures.

Power is the next parameter that is investigated as it relates to etching rate and sidewall profile. It was found that power was the main determining factor of etching rates in RIE of ChG films. The authors showed that the ionization of the CHF_3 gas saturates at a coil power of 400 W, as shown in Fig. 6 [20].

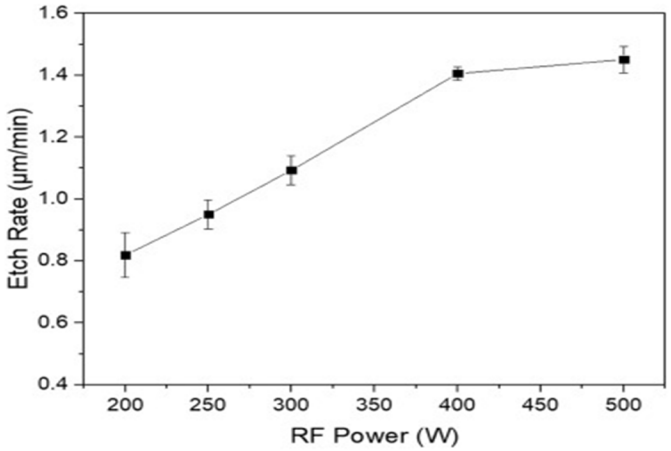

Fig. 6 — Etch rate as a function of coil power [20]

The anisotropy of the etch increases in a similar manner with power. After a power of 400 W is reached, the positive slope becomes very shallow. In addition, powers above 400 W may add unnecessary heat that may have adverse effects on the process. It is therefore recommended that a coil power of 400 W be used.

The authors go on to show the results of varying the gas flow rate. The etching rate and angle of the sidewalls are studied as functions of the gas flow rate, just as was done with coil power. The results differ from that of coil power, showing a more complex relation between gas flow and the results.

Keeping all of the other parameters constant (pressure of 3.75 mTorr and coil power of 300 W), the gas flow rate was varied between 10 sccm to 50 sccm in intervals of 10 sccm. As shown in Figure 7, the etching

rate increased for flow rates from 10 sccm to 20 sccm, and then showed a gradual decrease from 20 sccm to 50 sccm.

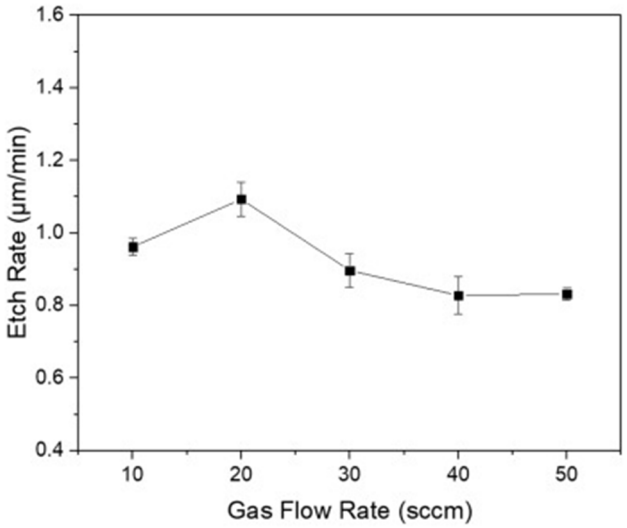

Fig. 7 — Etching rate as a function of gas flow rate [20]

The authors explain this phenomenon by stating that the increased etch rate for the flow rates of 10 to 20 sccm are easily accounted for by an increase in CHF_3 concentration and therefore an increase in chemical activity in the etching process. The decrease, though, is explained by the increase in gas flow speed causing a convection current that reduces the time the radicals and plasma actually interact with the surface, ultimately decreasing the etch rate.

The trend between gas flow rate and anisotropy differs from its relation to etching. The sidewall angles decrease constantly with increasing flow rate, as shown below in Figure 8. This is more easily accounted for by the fact that a higher flow rate results in a more chemically reactive process, which is inherently isotropic. Therefore, to optimize the anisotropy, one should maintain as low a gas flow rate as possible. It is therefore recommended that a rate of 20 sccm be used for chalcogenide glasses.

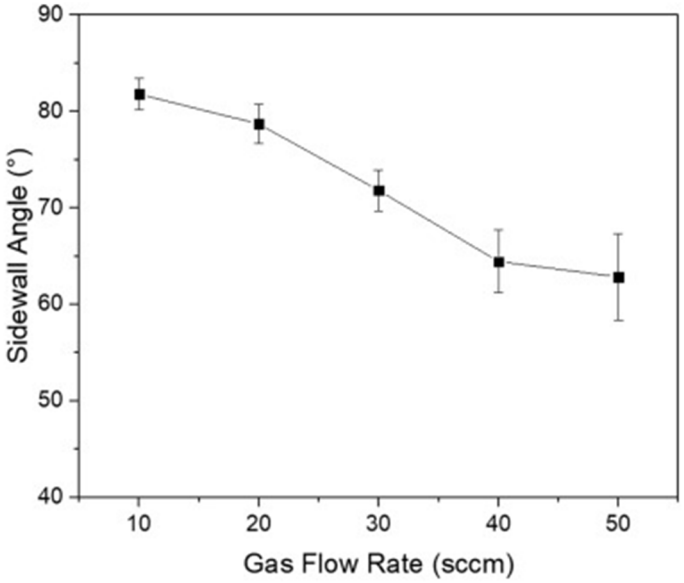

Fig. 8 — Sidewall angle as a function of gas flow rate [20]

Finally, chamber pressure is the last important factor that controls the plasma density and therefore has major effects on the anisotropy and the rate of the etching process. The authors originally studied the correlation between pressure and these results in terms of pascals. In order to keep a sense of consistency, these graphs have been translated into terms of mTorr.

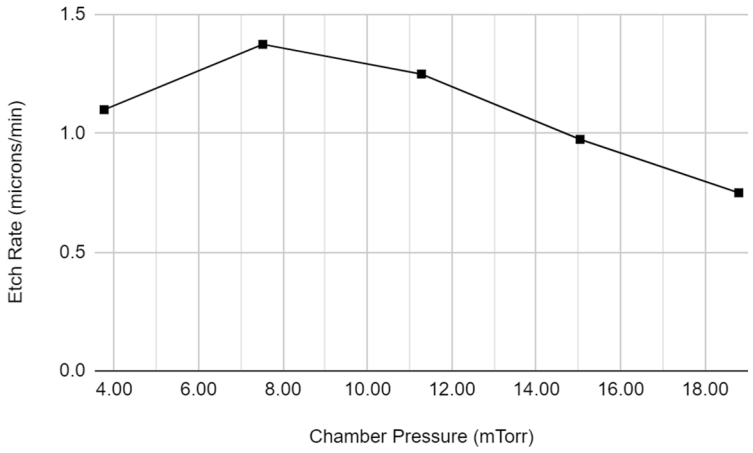

Fig. 9 — Etch rate as a function of Chamber Pressure [20]

We can see in Figure 9 that the etching rate peaks at a pressure value of 7.5 mTorr. The authors state that the initial increase in etching rate from 4 mTorr to 7.5 mTorr is simply because of an increase in plasma

density. The constant decrease that follows after, though, is explained by the higher concentration of gas present in the chamber. As the chamber pressure increases, the gas concentration increases, and this causes many collisions between the gas and the ions and electrons present in the plasma. This reduction in the mean free path of the ions and electrons effectively results in a lower etching rate.

The anisotropy of the etch has a constant decrease with increasing chamber pressure. This is, again, due to the collisions between the increasing gas concentration and the reactive ions. The increased concentration of gas scatters the ions so that they lose their directionality, which leads to more isotropic structures.

Another, most notable, effect of higher chamber pressures is the formation of a grass-like residue on the surface of the substrate. The authors explain that this is due, once again, to the higher concentration of gas present at higher pressures. Since more CHF_3 molecules are present within the chamber, then there will be more CF_x radicals that will be formed. These fluorocarbons will then deposit onto the surface and will prevent ion bombardment. In effect, these deposits will act as micromasks that will cause an uneven etching of the surface and will therefore form grass-like residues [20].

3.2.2 Phosphate Glass

A limited study of the etching of phosphate glasses was performed by Metwalli et al. [19]. The etching process for phosphate glass is unlike that of silicate glasses, or even chalcogenide glasses. Phosphate glasses are more susceptible to high etching rates when exposed to sputtering processes rather than ion assisted etching.

IOG glass is the specific type of phosphate glass that is being used in this study. IOG is reported to have a composition of 69% P_2O_5 and 31% mix of Na_2O, La_2O_3, and Al_2O_3. This glass is valuable because of its waveguide capabilities, especially in the short infrared region.

The authors of this study compared IOG glass to other more common glasses, such as silica and soda lime glass. Like previous studies, they varied the parameters for each of these glasses and reported the effects of each glass. In a first trial, the authors used Ar to etch the glasses while varying the coil power. IOG, above all other glasses, had the largest change with an increase of power in Ar plasma. Additionally, IOG glass had the overall highest etch rate in Ar plasma.

In a further trial, they placed the glasses in a chamber of CF_4/CHF_3 plasma. Keeping all the other parameters constant, they varied the ratio of CF_4 and CHF_3 in order to see if each glass shared a similar correlation to the change in gas concentration. They expected that each glass would show a decrease in etching rate as the ratio became more CHF_3 dominant. However, when they performed this trial on the IOG glass, they found almost no difference in etching rate as they varied the ratio.

Due to these two observations of IOG glass in RIE conditions, it was concluded that the mechanisms used to etch IOG glass, and phosphate glass in general, differ greatly from those that are used for silica based glasses. The authors claim that the lower binding energies of the "network and modifier species at the phosphate glass surface" are responsible for these differences. The fluorocarbon plasmas are simply not as effective as the Ar plasma, indicating that only a purely physical sputtering process is occurring in the etching of IOG glass. This is further proven when the CF_4/CHF_3 ratio is varied. The lack of change under these altering conditions further suggests that it is not a chemical process at all [19].

To the best of our knowledge, there does not appear to be any research that explicitly states what other conditions would optimize the etching rate of phosphate glasses. However, it may be inferred from previous

studies that a larger plasma density and a limited gas concentration would allow for optimal etching conditions. Therefore, a high coil power that would saturate the plasma fully, along with a low pressure and relatively low gas flow rate would all contribute to a high etching rate. This would maximize the density of the Ar plasma and would avoid instances of diffuse scattering. This would likely result in a fairly anisotropic etching result as well.

3.2.3 Titanium Oxide Glass

Many high index glasses contain high concentrations of TiO_2. There is not significant research that has been conducted on RIE of specific TiO_2 containing glasses. However, preliminary research has been performed on TiO_2 thin films. The results show lower etch rates as compared to previously mentioned glasses. Currently, one of the highest reported etching rates for pure TiO_2 is 140 nm/min using a SF_6/Ar gas mixture [21].

One study performed by Hotovy et al [22] provides some interesting results concerning the reactive ion etching of TiO_2. An array of Au nanoparticles were applied to a TiO_2 substrate to prepare it for RIE patterning. A mixture of CF_4 and Ar were used in this process, with flow rates of 4 sccm and 10 sccm, respectively. This was powered by an RF generator at 13.56 Hz with a coil power of 200 W. Additionally, the chamber pressure was set at 4.5 mTorr. The authors of this study were particularly interested in varying the platen power, increasing the power from 0-150 W in intervals. At 150 W, the highest etching rate achieved of TiO_2 was reported to be 93 nm/min.

The largest reason for this low etching rate is the formation of TiF_3, the nonvolatile product of CF_4 and TiO_2. With its melting point standing at 2000^{o}C, it is no easy feat to remove it from the surface of the substrate. The authors, however, point towards a clever solution to overcome this issue. They suggest that

the flow rate of Ar be increased. They believe that if this is sufficiently increased, then the number of radicals will increase, which would mean that there would be a higher concentration of F^- present. If this were to happen, then the free F^- would be able to react with the TiF_3 particles. This would result in the formation of TiF_4, which happens to have a much lower boiling point and would be much easier to remove from the surface. In this, the authors place hope in the future of etching TiO_2 [22].

Interestingly, the authors [22] made use of a layer of gold nanoparticles as micro-masks on the surface of the TiO_2.

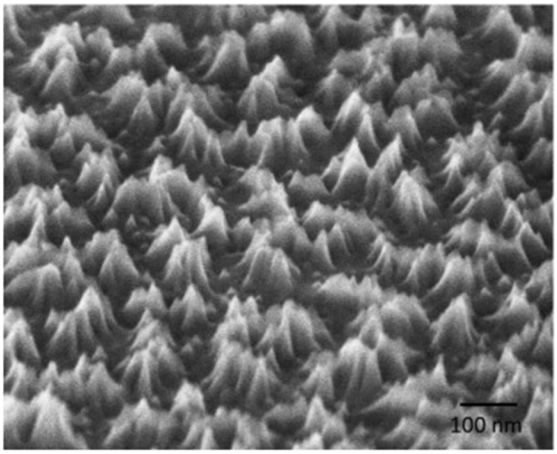

Fig. 10 — SEM image of etched nanostructures on TiO_2 surface after using an RF platen power of 100 W for 2 minutes [22]

These nanoparticles allow for these nanostructures to be formed. The locations of the nanoparticles correspond to the peaks of the structures, while the valleys correspond to the gaps between the particles. These results indicate that pure TiO_2 is susceptible to etching rARSS. However, more research must be conducted in order to verify whether TiO_2 containing glasses would yield similar results [22].

4. FORMATION OF rARSS ON GLASS

Having discussed the optimization of parameters that are necessary to conduct ICP-RIE processes on various glasses, it is now possible to realize how this may aid in an understanding of what is necessary to fabricate ARSS. In order to fully understand how these structures are made, we will begin with a discussion of how ordered ARSS are made. It will be shown how they are designed and how they improve light transmission. Following this, a detailed account of how they are fabricated will be related. Then, rARSS will be explored. We will then describe methods that have been shown for fabricating rARSS. Finally, examples of creating rARSS on specific glasses will be presented.

4.1 Formation of ARSS

The need for ARSS has risen recently in the world of AR optical surfaces. AR technology has mostly been achieved using AR thin films deposited on the surface of a substrate [30]. This involves the creation of destructive interference of any reflected rays through the use of this coating. There are, however, three main issues with this method. First is that this method is specific to a range of wavelengths, since the refractive index of the film may not allow for destructive interference at a wide range of wavelengths. Some have addressed this issue by depositing multiple layers that allow for a more broadband effect, but this is a very complex task and can be quite expensive. Second, there are some materials with high refractive indices that would not have a coating that could be sufficiently high enough index to allow for the needed interference effect. Third, these coatings cannot be fully utilized for some applications because the laser damage threshold for these coatings can be quite low. Therefore, although AR coatings can be quite effective at increasing transmittance to very high levels, they do not always meet demanding application requirements.

Thus, ARSS are an alternative solution that theoretically could reach these same levels of light transmittance for large ranges of wavelengths while being capable of fabrication on various substrates.

So, what exactly is ARSS? ARSS are a series of repeated nanostructures that are smaller than the wavelength of light for a given band of interest. These structures were originally inspired by nanostructures that were observed to be present on the surface of moth eyes [23]. The AR properties of moths' eyes made them less susceptible to being noticed by predators. Thus, these repeated AR surface structures are often called "moth eye" structures. ARSS prevent reflection of light by the use of geometry rather than distinct layers of other materials in AR coatings. These structures provide for a gradual change in the index of refraction between air and the substrate, reducing the Fresnel reflection in comparison with that of a smooth surface.

The method by which ordered, patterned ARSS are made is achieved through a series of tasks. First, a layer of photoresist is deposited onto a substrate through spin coating. Then, the substrate is placed under a pre-fabricated, patterned photo mask and is exposed to UV light. This chemically altered photoresist is selectively removed using a liquid etch. Finally, the substrate with the patterned photoresist is placed into an ICP-RIE device to transfer the pattern into the sample's surface [31].

A handful of alternative methods not requiring the photoresist have also been developed. One such method is the one developed by Xin Ye and his group [5]. They deposited a layer of ordered polystyrene nanoparticles on the surface of the substrate to form a pattern. This layer acted as a substitute for the photoresist. This method was especially interesting because they could stop the RIE process at various periods of time, and they could form different shapes of structures, which would have slightly different values of reflectance.

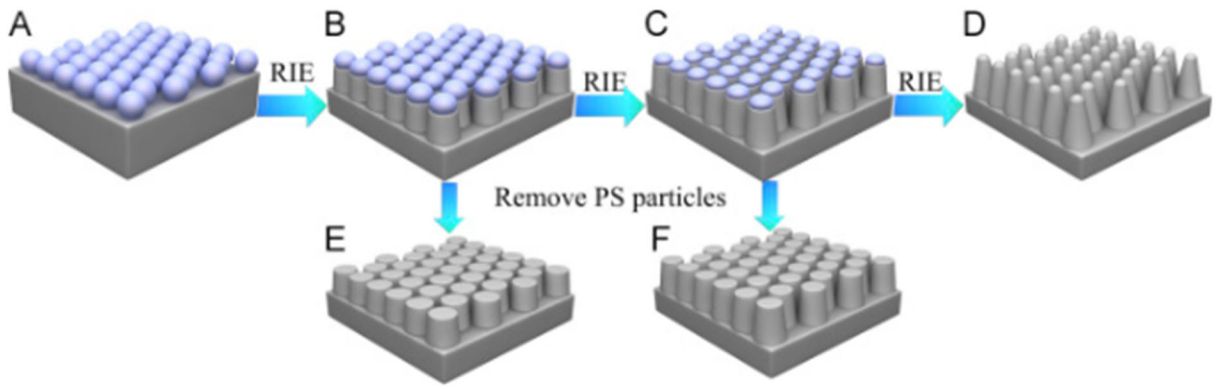

Fig. 11 — Shape of nanostructures as a function of etching time with PS nanoparticle masking layer [5]

These structures can vary from being pillar shaped to paraboloid shaped. This is, undoubtedly, an interesting method of fabrication [5]. It is, however, still very complex to be able to form a distinct pattern on the substrate. These methods become more difficult when attempted on curvilinear substrates [23].

ARSS has many advantages over AR thin films. It eliminates the need for films of different materials that have refractive indices appropriate for a given substrate, and instead require only a geometric change to the surface of the substrate. In addition, ARSS has demonstrated the ability to withstand high energy laser irradiance, increasing the suitability for many applications where thin film coatings would not be successful [23]. However, we note that the ways to form these regularly patterned "'moth eye'" structures can be quite complex and tedious. There are advantages for rARSS, or random anti-reflective surface structures, as a type of ARSS with no well-defined pattern or regularity either in the spacing between each structure or in the shape or height of the structures themselves [23].

4.2 Formation of rARSS

There are three main methods of fabricating rARSS on glass substrates [24]. The first method is to deposit a thin layer of metal, usually gold or silver, onto the surface of the substrate. Then, the gold is annealed at a high temperature to form local islands of metal to mask the substrate. Following, the coated substrate is dry etched and forms grass like structures in the exposed parts of the substrate. The second method of forming rARSS is doing a two-step process without forming a formal mask prior to dry etching. The first step is to dry etch the substrate directly. Then the passivation phase begins. This phase is paused, and the gas is allowed to react with the surface. At this point a polymer film will form on the surface, and this will act as a masking layer to unevenly etch the surface, again making rARSS. The third method is a one step process of etching the surface directly with no pauses. This method relies heavily on the amorphous structure of the glass. The hope is that any irregularities in the amorphous structure will be exaggerated through dry etching, which will result in random ARSS on the surface [24].

4.2.1 rARSS of Fused Silica

Recent research on rARSS fabrication on glass has primarily focused on fused silica. In this section, we will discuss the three methods mentioned above and go into greater detail regarding the parameters used in each instance. Hopefully, this can give a full understanding of the conditions necessary to form rARSS.

The first method, as discussed above, is to deposit a layer of metal on the surface, such as Au or Ag [25]. The purpose of this is to, in some way, mask the surface so as to promote the growth of surface structures. This “masking” occurs in a very interesting way, not acting as a mere physical barrier. An electrostatic sheath is generated during RIE processes wherein an electric field is generated perpendicular to the substrate surface. When metal features are formed on top of the insulative silica, they create metallic/insulator interfaces where the two materials meet. These interfaces interact strongly with the generated electric field.

Thus, the ions present in the plasma are drawn especially to these regions. This is why metals such as gold and silver are used in rARSS etching processes [25].

Looking into a specific example of this process, we turn to a study performed by Zhao et al. [26]. In order to create rARSS, they first deposited 5-10 nm of Ag via sputtering. Then they rapidly annealed the Ag at 200°C, forming nanopatterns through the dewetting process.

After preparing the sample, the substrate was then placed into an RIE chamber. The main reactant gas used was CHF_3, and it was charged at an ion energy of 400 eV. The ion current was 110 mA, and the pressure of the plasma was set to 8.25×10^{-5} Torr. The substrate was then removed from the etching chamber and placed into a nitric acid solution to eliminate the remaining Ag nanoparticles. The results of this particular study were shown to increase the transmittance by 3% for a one-sided etch [26].

The second example found is a research study performed by Rajendra Joshi at the University of North Carolina, Charlotte [27]. He implemented the two step process, alternating between etching and passivation steps, in order to create polymer layers that would block the non-etched layers. He used SF_6 as the main processing gas and then used C_4F_8 in the passivation steps. He notes that the C_4F_8 is vital to the passivation step because it decomposes into $(CF_2)_n$ radicals which then diffuse onto the surface, forming some sort of polymer layer (saying it is similar to Teflon).

Table 6 — 2-step Etching Parameters of Fused Silica [27]

Parameter	**Passivation**	**Etching**
C_4F_8 flow (sccm)	85	0
SF_6 flow (sccm)	0	130
O_2 flow (sccm)	0	13
Cycle Time (Seconds)	7	9

Platen Power (Watts)	0	Variable
Coil Power (Watts)	Variable	
Chamber Pressure (mTorr)	Variable	
Etching Time (Minutes)	Variable	

The parameters listed in Table 6 are ones he initially started with to perform deep reactive ion etching. These parameters are not yet set up to achieve optimal transmission, only to etch deeply and anisotropically.

Using these parameters as a starting point, Joshi then varied the platen and coil powers, as well as the etching time and chamber pressure. He correlated the average roughness of the rARSS with the transmissivity of the etched sample. Thus, whatever parameters increased the roughness of the sample, generally were found to lead to better results.

After varying all of the parameters, Joshi came to the following conclusions. First the roughness can only be fully optimized for certain ranges of wavelengths. Although rARSS did provide for desirable broadband AR performance, the wavelength regions with lowest reflectance were found to depend on the process conditions.

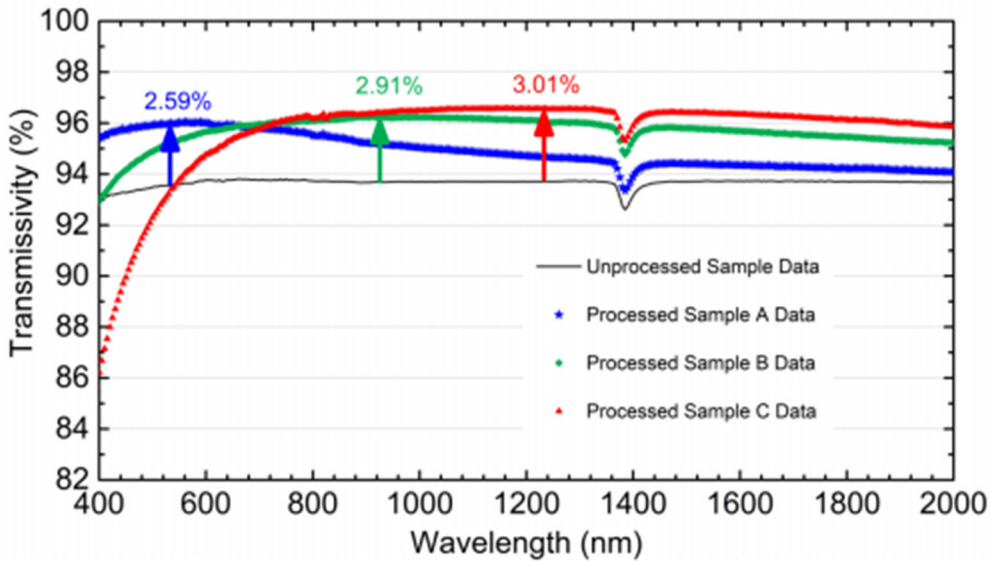

Fig. 12 — Transmissivity versus wavelength of three rARSS treated samples.
Sample A Parameters: 15 W Pl. Power, 500 W Coil Power, 15 mTorr Pressure, 30 min.
Sample B Parameters: 30 W Pl. Power, 750 W Coil Power, 30 mTorr Pressure, 60 min.
Sample C Parameters: 45 W Pl. Power, 1000 W Coil Power, 45 mTorr Pressure, 90 min. [27]

As shown in Fig. 12, for optimum blue/violet light transmission, Joshi showed that the parameters used should be 15 W for the platen power, 500 W for the coil power, 30 mTorr chamber pressure, and it should be etched for 30 min. This increased the transmission by about 2.6% (compared to the untreated sample) for wavelengths ranging from 400-700 nm. These results correlated to an average measured roughness of ~20 nm. The parameters required to improve transmission at wavelengths of 800 nm and above were much more intense. The platen power was set to 45 W, the coil power was set to 1000 W, the chamber pressure of 45 mTorr was used, and etching was performed for a 90 minute period. This resulted in a roughness of ~150 nm, improving the transmission by 3% for wavelengths greater than 800 nm.

In addition to the spectrophotometer results, an analysis was performed using an ellipsometer. This was done in order to determine the transmissivity as a function of the angle of incidence. Sample C, which had ARSS specifically fabricated for high IR transmission, showed enhanced performance as long as the AOI was below 45 degrees (for s-polarized incident light), and remarkably, there was little change in

transmission with angle for Sample C when compared to the unprocessed glass for AOI up to 60 degrees for p-polarized light.

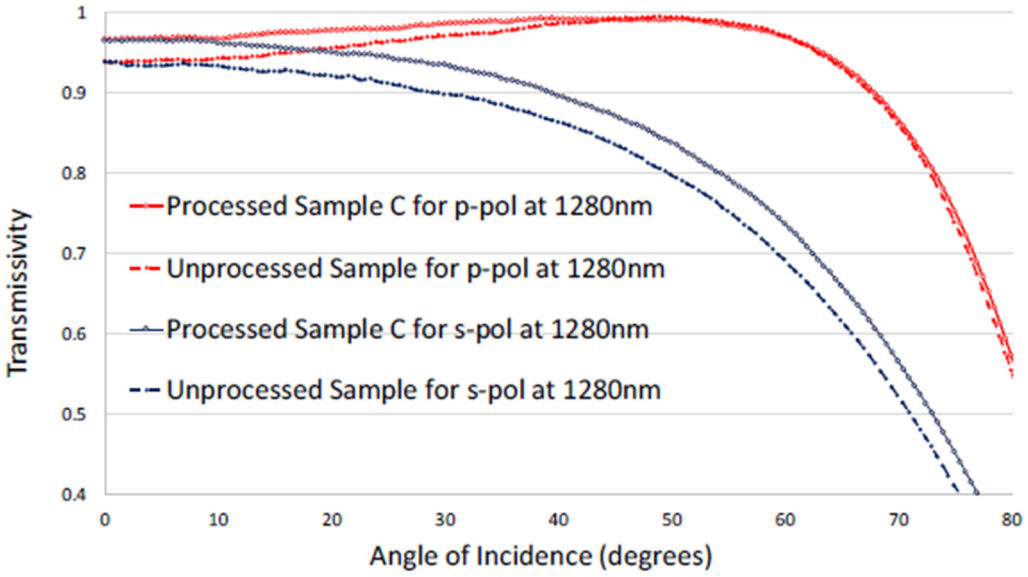

Fig. 13 — Ellipsometric measurements showing transmissivity as a function of AOI [27]

As a final note, Joshi included a more detailed account of how he calculated the roughness of the samples. He used a simple average (R_a), a root-mean square (R_q), and a sum of the minimum and maximum height values (R_z). He also measured the skew and kurtosis of the peaks in order to give a detailed account of the structures being made under the changing conditions. A skewness value of 0 indicates a privation of skew, a value less than 0 indicates a skew to the left, while a value greater than 0 indicates a rightward skew. The kurtosis describes the shape of the structure. A value of 3 indicates a Gaussian distribution, a value less than 3 indicates a semicircular shape, while a value greater than 3 indicates a sharper point of the curve. Joshi then presented how each parameter may affect each of these values in the following tables [27].

Table 7 — Change in roughness parameters with changes in chamber pressure [27]

Sample	Roughness				
	R_a (nm)	R_q (nm)	R_z (nm)	R_{sk}	R_{ku}
Unprocessed	3.5	4.4	30.1	0.06	2.97
Processed (15 mTorr)	22.61	28.02	153.14	0.17	2.57
Processed (30 mTorr)	121.88	151.35	780.18	0.08	2.72
Processed (45 mTorr)	148.32	183.07	1007.26	0.07	2.77

Table 8 — Change in roughness parameters with changes in platen power [27]

Sample	Roughness				
	R_a (nm)	R_q (nm)	R_z (nm)	R_{sk}	R_{ku}
Unprocessed	3.5	4.4	30.1	0.06	2.97
Processed (15 Watt)	98.52	119.72	633.71	-0.09	2.40
Processed (30 Watt)	121.88	151.35	780.18	0.08	2.72
Processed (45 Watt)	149.29	187.47	1007.59	0.13	2.30

Table 9 — Change in roughness parameters with changes in coil power [27]

Sample	Roughness				
	R_a (nm)	R_q (nm)	R_z (nm)	R_{sk}	R_{ku}
Unprocessed	3.5	4.4	30.1	0.06	2.97
Processed (500 Watt)	91.34	113.51	608.45	-0.21	2.91
Processed (750 Watt)	121.88	151.35	780.18	0.08	2.72
Processed (1000 Watt)	152.75	192.08	948.56	0.35	2.95

Table 10 — Change in roughness parameters with change in etching time [27]

Sample	Roughness				
	R_a (nm)	R_q (nm)	R_z (nm)	R_{sk}	R_{ku}
Unprocessed	3.5	4.4	30.1	0.06	2.97
Processed (30 Minute)	39.65	49.79	267.59	0.27	2.93
Processed (60 Minute)	121.88	151.35	780.18	0.08	2.72
Processed (90 Minute)	139.06	168.76	907.52	0.38	2.69

Finally, we turn to the final method of etching rARSS, etching directly onto the substrate with no mask. Lilienthal et al [28] performed an interesting study where they investigated the effects of parameters in RIE and compared results in processes performed with a passivation step to those that did not on samples of fused silica. The main focus of the study was to characterize the different geometries of the structures formed and the packing densities of the structures.

The first observation made by this group is that given different sets of conditions, four basic types of structures can be fabricated. The first category is the thinnest and has slightly sloped sidewalls and it is referred to as "glass grass." The other categories stray further away from these properties and trend towards being thicker and more anisotropic. These categories, in ascending order, are 'needles', 'pillars', and 'tubes'. Depending on the structure chosen, there will be different levels of packing density that will be possible to achieve with that structure, which limits the level of transmission that is possible [28]. Their goal of fabricating rARSS was to fabricate as small of a structure as possible to optimize the transmission of the desired wavelength spectrum. If this is accomplished, the authors state that the packing density may be maximized, further bolstering the effectiveness of rARSS [28].

The group used two basic sets of parameters, one for the two step Bosch process and one for the one step process. The two step process is identical to the one used by Joshi, and the other process is listed below in Table 11.

Table 11 — Parameters for one step etch of Fused Silica [28]

Parameter	**Process without passivation step**
C4F8 flow (sccm)	-
SF6 flow (sccm)	130
O2 flow (sccm)	13
Platen Power (Watts)	100
Coil Power (Watts)	600
Chamber Pressure (mTorr)	24
Chamber Temperature (°C)	20-30
Etching Time (Minutes)	10-180 (90 standard)

These parameters were used as a starting point from which the authors began to vary the parameters so as to study the effects these have on the diameter and packing density of the structures.

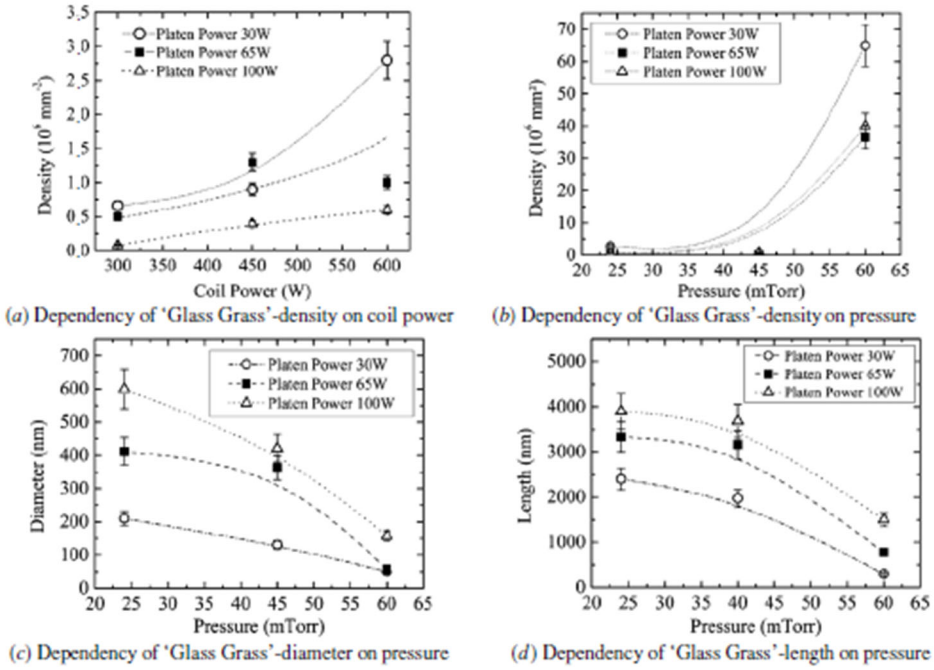

Fig. 14 — Density and size of surface structures as a function of coil power and pressure [28]

As can be seen in Figure 14, the general trend was that density increases with a decrease in platen power and an increase in coil power or pressure. The size of the structures themselves increased with platen power and decreased with pressure [28].

The research group also stated the following, which provides an interesting account of some details that may affect the structure of the rARSS:

> "There are several additional general plasma effects which can influence the morphology of etched micro- and nanostructures. Excessive ion energy or ion deflection from sidewalls can lead to the effect known as 'trenching'. Charging effects in dense areas can influence the profile shape creating a negative sidewall profile (bowing). 'Ion trajectory distortion' and 'undercutting' result from additional high ion energy, while 'notching' or 'footing' effects at dielectric interfaces can result from insufficient ion energy or high aspect ratios. Furthermore, sidewall passivation is the deposition of non-volatile reaction products on

vertical structures and is called ‘tapering’ when it is very distinct. This can assist determined or self-organized vertical microstructures” [28].

These results undoubtedly are useful in determining the parameters necessary to maximize the optical transmission of silica. From this study [28], it appears that SF_6 was their processing gas of choice, that the density and shape of the etched features affect the transmissivity of the final product, and that non-masking etching is the least practiced and least explored of the methods.

4.2.2 rARSS of Borosilicate Glass

The report on forming rARSS on borosilicate glass will be quite brief, as we found only one report of the process for this material. This procedure was performed by Cui et al. [29]. In this procedure, they used the first method, depositing a layer of silver on the surface and then using ICP-RIE.

To begin, they used a standard thermal evaporation process to deposit the silver layer on the substrate. The thickness of this film was varied to four different values in order to determine what thickness was most conducive to forming rARSS. Following this, the samples with silver layer were annealed at 200ºC for one hour in an N_2 oven.

After preparing the substrate with the silver masking layer, the sample was taken into the ICP-RIE. CF_4 gas was input into the system at 30 sccm for five minutes. The plasma was induced using a 40 W RF coil power and the pressure was kept constant at 50 mTorr. After the etching process, the sample was then placed into an HNO_3 bath for three minutes to remove any remaining Ag.

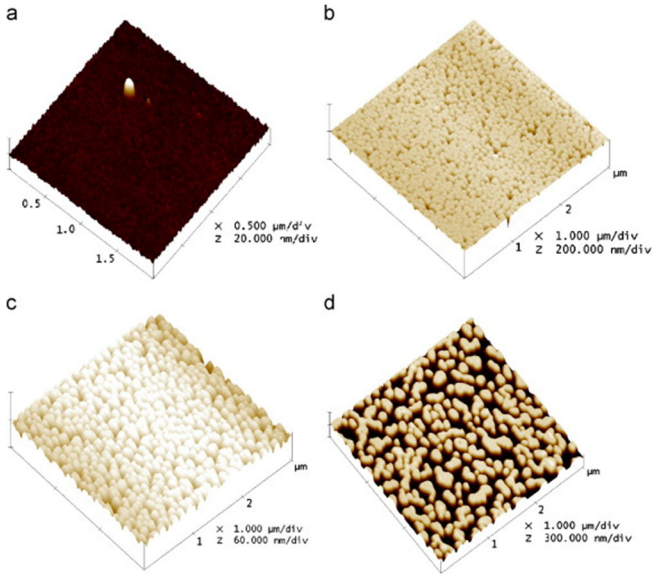

Fig. 15 — AFM images of subwavelength structured glass prepared using as-deposited Ag thickness: (a) 4 nm, (b) 8 nm, (c) 11 nm, (d) 15 nm [29]

Their AFM images in Fig. 15 show that the thickness of the Ag layer determined the Ag nanoparticle size, which in turn determined the size of the rARSS. As can be seen in the above image, an 8 nm layer did not maximize the size of the surface structures as much as the 11 nm layer. The 15 nm layer allowed for nanoparticles that are too large, which caused large gaps between the structures. Therefore, it would seem that an 11 nm layer produced the most ideal rARSS, which is confirmed by the spectrophotometry results shown Figure 16 [29].

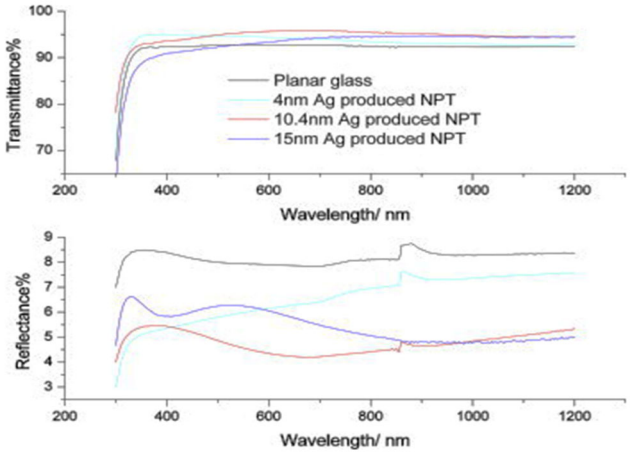

Figure 16 — Spectrophotometry results of the etched glasses [29]

5. RESULTS AND DISCUSSION

Having surveyed the results of many trials of ICP-RIE and rARSS processes, it comes time now to synthesize these results and analyze any trends. In this section, we will discuss all the variations of processes that were presented and summarize those found to be suitable for each glass material, including which processing gases and etch parameters that were found to be most suitable for each glass based on its chemical composition.

There were three main processes that were discussed in the rARSS section. The first method was to deposit and anneal a metal masking layer, typically Au or Ag, and then use a standard ICP-RIE process. The second method was to use a two-step method, alternating between etching and passivation. The third method was to do one continuous etching process. In addition to this, there is also a consideration of using a purely physical process (using only Ar plasma) or employing a combination of both chemical and physical processes.

Since using a masking layer is sometimes undesirable, we summarize only the last two methods. As described previously, an inert gas was often used to accompany a fluorine gas in order to combine the effects of chemical and physical etching.

It was found that fused silica would form rARSS using either of the following methods. First, a CF_4/Ar mixture can be used in the case of a single step, no-masking method. This allowed for constructive interference in two ways. The CF_4 makes chemical species that react with the silica, while the Ar physically bombards the surface, assisting in sensitizing the surface. At the same time, the Ar ions would backscatter some of the outgoing volatile species which would then redeposit on the surface. This resulted in a successful method for forming rARSS [3, 28]. In the second case, etching with a SF_6/Ar mixture followed by a C_4F_8 gas used in the passivation step created a similar effect to the previous method. SF_6 was shown

to be a more reactive species with SiO_2 than CF_4, which allows for faster etching rates. By switching between these two process steps, it is possible that more anisotropic structures are obtained, due to formation of a quasi-polymer layer on the surface [27]

The general rules to enhance the etching rate for SiO_2 included using the highest possible coil power that does violate a level of tolerance of isotropy. The chamber pressure was set as low as possible without sacrificing the striking of the plasma itself, in order to give a flow rate of processing gas that saturates the plasma but does not reduce the mean free path of the ions. Finally, the proportion of Ar to the chemical species of gas was about 1:3, which avoided the process to be dominated by physical sputtering.

In a number of the studies presented, it was shown that a high bias voltage is necessary to perform deep features using RIE. However, since the electrode spacing was not indicated in these studies, the effective electric field produced may have varied drastically. While it can be stated that a high bias voltage is generally good, no specific range of voltages was confirmed, since a very different electric field could occur depending on the geometric specifics of the equipment on hand. However, based on the literature results, it was found that any conditions that increased bias voltage resulted in a quicker etching rate.

As was shown in the study performed by Lilienthal et al [28], the platen power was kept low, at around 10 W when forming rARSS in SiO_2. The pressure and coil power may also vary with the desired area density and size of the structures desired. Using a higher pressure of around 50 mTorr resulted in a decrease of the etching speed, but it also increased the concentration of the processing gas, which is then given the opportunity to form radicals which will then redeposit on the surface. This resulted in formation of more surface structures, but they were not as wide or as deep as the features made under low pressure conditions. A similar effect is observed when rARSS was fabricated using high coil powers, especially those that approach 1 kW [28].

The following summary of etching parameters were reported for pure TiO_2. A low pressure of 4.5 mTorr was used, with a 200 W coil power and a 150 W platen power. The etching rate is limited by the desorption of the nonvolatile product, TiF_3. It was reported that an overabundance of Ar being supplied during the process may form excess F^- ions which could react with the TiF_3 to form TiF_4 which is a volatile product [22].

Phosphate glasses are reported to have almost no chemical character that suitably reacts with a fluorine gas [20]. The binding energies of the "network species" present on the surface are said to be the cause of this lack of chemical activity. For this glass, it was recommended that Ar be the primary gas used. CF_4 or C_4F_8 were also implemented as well, in order to create polymer layers during etching [19, 20].

The chalcogenide glass etching that was reported here, for $Ge_{20}Se_{75}Sb_5$, showcased a peculiar reaction to RIE. It actually etched too quickly under conditions similar to those for silicate glasses, approaching 2 μm/min. In order to reduce this, the coil power was lowered to 400 W, with a flow rate of 40 sccm for a mixture of CHF_3 and O_2. CHF_3 was used because it is not as reactive as CF_4, and the O_2 was used because it is was reported to dilute the chemical activity of the fluorine gas while also contributing to the physical sputtering [20].

Some other interesting observations were made in this study [20] of etching ChG glasses. The first was that a balance must be kept for each parameter, with radical values negatively affecting the quality of the etch. First, a flow rate of 20 sccm was recommended because a lower one did not give a strong enough concentration to effectively etch the surface, while a higher one caused a convection current which decreased the time of contact between the ions and the substrate. Second, a pressure of 7 mTorr was recommended for deep etching because a lower pressure resulted in a much lower plasma density, while a higher one caused collisions and scattering which leads to isotropy and lower etching rates. It was also

observed that a higher pressure led to formation of grass-like structures, which appear similar to random ARSS [20].

In conclusion, we have discussed the optimal reactive ion etching parameters for different types of glasses, and described published research for how these parameters were adjusted in specific instances to form random AR surface structures on silica glasses. Our intention for this report is that it may aid in an improved understanding of the parameters necessary to etch many different types of glass materials, utilizing ICP-RIE methodology.

REFERENCES

1. "Stanford Nanofabrication Facility: Dry Etching." Lecture Series by James McVittie, *Stanford Nanofabrication Facility*, 7 Dec. 2016, www.youtube.com/watch?v=UMvRXF3ZZr4.

2. Leech, Patrick W. *Reactive Ion Etching of Quartz and Silica-Based Glasses in CF_4/CHF_3 Plasmas.* Vacuum, 55 (3–4) (1999), pp 191-196.

3. Schmitt, Jana, et al. *Reactive Ion Etching (CF_4/Ar) and Ion Beam Etching of Various Glasses for Diffractive Optical Element Fabrication* International Journal of Applied Glass Science, 9 (4) (2018), pp. 499-509.

4. Zhang, Chenchen, and Srinivas Tadigadapa. *Modified Inductively Coupled Plasma Reactive Ion Etch Process for High Aspect Ratio Etching of Fused Silica, Borosilicate and Aluminosilicate Glass Substrates.* Sensors and Actuators A: Physical 273 (2018), pp 147-158.

5. Ye, Xin, et al. *Subwavelength Structures for High Power Laser Antireflection Application on Fused Silica by One-Step Reactive Ion Etching.* Optics and Lasers in Engineering 78 (2016), pp. 48-54.

6. T. Abe, M. Esashi *One-chip multichannel quartz crystal microbalance (QCM) fabricated by deep RIE* Sens. Actuators A: Phys., 82 (1) (2000), pp. 139-143.

7. X. Li, T. Abe, M. Esashi *Deep reactive ion etching of pyrex glass using SF_6 plasma,* Sens. Actuators A: Phys., 87 (3) (2001), pp. 139-145.

8. W. Chen, K. Sugita, Y. Morikawa, S.Yasunami, T. Hayashi, T. Uchida *Application of magnetic neutral loop discharge plasma in deep silica etching* J. Vac. Sci. Technol. A: Vac. Surf. Films, 19 (6) (2001), pp. 2936-2940.

9. S. Queste, R. Salut, S. Clatot, J.-Y. Rauch, C.G.K. Malek *Manufacture of microfluidic glass chips by deep plasma etching, femtosecond laser ablation, and anodic bonding,*Microsyst. Technol., 16 (8–9) (2010), pp. 1485-1493.

10. C. Zhang, G. Hatipoglu, S. Tadigadapa *High-speed ultrasmooth etching of fused silica substrates in SF_6, NF_3, and H_2O-based inductively coupled plasma process,* J. Microelectromech. Syst., 24 (4) (2015), pp. 922-930.

11. M.J. Ahamed, D. Senkal, A.A. Trusov, A.M. Shkel *Study of high aspect ratio nld plasma etching and postprocessing of fused silica and borosilicate glass,* J. Microelectromech. Syst., 24 (4) (2015), pp. 790-800.

12. Vieillard, Julien, et al. *Integrated Microfluidic–Microoptical Systems Fabricated by Dry Etching of Soda-Lime Glass* Microelectronic Engineering, 85 (2) (2008), pp. 465-469.

13. T. Ichiki, Y. Sugiyama, T. Ujiie, Y. Horiike *Deep dry etching of borosilicate glass using fluorine-based high-density plasmas for microelectromechanical system fabrication,* J. Vac. Sci. Technol. B: Microelectron. Nanometer Struct. Process. Meas. Phenom., 21 (5) (2003), pp. 2188-2192.

14. J.H. Park, N.-E. Lee, J. Lee, J.S. Park, H.D. Park *Deep dry etching of borosilicate glass using SF_6 and SF_6/Ar inductively coupled plasmas,* Microelectron. Eng., 82 (2) (2005), pp. 119-128.

15. T. Akashi, Y. Yoshimura *Deep reactive ion etching of borosilicate glass using an anodically bonded silicon wafer as an etching mask,* J. Micromech. Microeng., 16 (5) (2006), p. 1051.

16. H.C. Jung, W. Lu, S. Wang, L.J. Lee, X. Hu *Etching of pyrex glass substrates by inductively coupled plasma reactive ion etching for micro/nanofluidic devices,* J. Vac. Sci. Technol. B: Microelectron. Nanometer Struct. Process. Meas. Phenom., 24 (6) (2006), pp. 3162-3164.

17. A. Goyal, V. Hood, S. Tadigadapa *High speed anisotropic etching of pyrex for microsystems applications* J. Non Cryst. Solids, 352 (6) (2006), pp. 657-663.

18. K. Kolari *Deep plasma etching of glass with a silicon shadow mask,* Sens. Actuators A: Phys., 141 (2) (2008), pp. 677-684.

19. Metwalli, EzzEldin, and Carlo G. Pantano, *Reactive Ion Etching of Glasses: Composition Dependence*, Nuclear Instruments and Methods in Physics Research Section B: Beam Interactions with Materials and Atoms 207 (1) (2003), pp. 21-27.

20. Xiong, Hao, et al. *Reactive Ion Etching of Ge-Sb-Se Ternary Chalcogenide Glass Films in Fluorine Plasma,* Microelectronic Engineering (225) (2020), 111259.

21. Norasetthekul, S., et al., *Dry Etch Chemistries for TiO2 Thin Films* Applied Surface Science, 185 (1–2) (2001), pp. 27-33.

22. Hotovy, I., et al. *Dry Etching Characteristics of TiO_2 Thin Films Using Inductively Coupled Plasma for Gas Sensing,* Vacuum 107 (2014), pp. 20-22.

23. Busse, Lynda E., et al. *Review of Antireflective Surface Structures on Laser Optics and Windows,* Applied Optics 54, (31) (2015) pp. F303-F310.

24. Peltier, Abigail, et al., *Control of Spectral Transmission Enhancement Properties of Random Anti-Reflecting Surface Structures Fabricated Using Gold Masking*, Proc. of SPIE Vol. 10115, (2017), pp. 10115B-1-7.

25. Lohmueller, Theobald, et al., *Improved Properties of Optical Surfaces by Following the Example of the "Moth Eye"*, Biomimetics Learning from Nature, Amitava Mukherjee (Ed.), ISBN: 978-953-307-025-4, (2010) InTech, pp. 451-463.

26. Zhao J, Qi H, Wang H, He H, Zhang W. *Scattering analysis for random antireflective structures on fused silica in the ultraviolet*. Opt Lett. 40 (22) (2015), pp 5168-5171.

27. Joshi, Rojendra. *Fabrication, Characterization, and Modeling of Random Antireflective Optical Surface Structures*, Ph.D Thesis, The University of North Carolina at Charlotte, 2020.

28. Lilienthal, Katharina, et al., *Fused Silica "Glass Grass": Fabrication and Utilization, Journal of Micromechanics and Microengineering* 20 (2) (2010), p. 025017.

29. Cui, Hongtao, et al., *A Novel Silver Nanoparticle Assisted Texture as Broadband Antireflection Coating for Solar Cell Applications,* Solar Energy Materials and Solar Cells 109 (2013), pp. 233-239.

30. Nole, Jim, *Nanotextured Optical Surfaces Advance Laser Power and Reliabilit,.* Optical Materials, Laser Focus World, 9 June 2014, www.laserfocusworld.com/optics/article/16550179/optical-materials-nanotextured-optical-surfaces-advance-laser-power-and-reliability.

31. MacLeod, Bruce D., and Douglas S. Hobbs, *Low Cost Anti-Reflection Technology For Automobile Displays,"* TelAztec (Oct. 2004): telaztec.com/Resources/SID-ME-AutoDisplayOct04.pdf.